Volume 14, Number 2, 2021. pp. 101-109

Jordan Journal of Physics

ARTICLE

Structural and Optical Characterization of Thermally Oxidized Titanium Thin Films Prepared by Ion Beam-assisted Deposition (IBAD) Technique

N. Hamdadou[a] and **I. M. Odeh**[b]

[a] *Laboratoire de Micro et de Nanophysique (LaMiN), Ecole Nationale Polytechnique d'Oran (ENPOran), BP 1523 El Mnaouer, Oran 31000, Algeria.*

[b] *Physics Department, Yarmouk University, Irbid 21163, Jordan.*

Doi: **https://doi.org/10.47011/14.2.1**

Received on: 28/10/2019; *Accepted on: 11/06/2020*

Abstract: Titanium oxide (TiO_2) thin films have been grown by thermal oxidation of sputtered Titanium (Ti) thin layers using ion beam-assisted deposition (IBAD). X-ray diffraction showed that prior to oxidation, the films are composed of hexagonal crystallites of Ti. After oxidation, a film structure transition occurs from monoclinic β-TiO_2 type to tetragonal anatase type as the annealing temperature of Ti layer is increased from 250 °C to 550 °C. The film thickness was about 230 nm. Visualization and scanning by atomic force microscope (AFM) revealed a low roughness of the samples, which increases when the annealing temperature is increased. The optical transmittances of the films in the visible spectrum were in the range of 85-95%. The values of optical band gap have been estimated to be 3.43 eV and 3.61 eV, for thin films annealed at 250°C and 550°C, respectively.

Keywords: TiO_2 thin film, IBAD, XRD, Structural and optical properties.

Introduction

Due to the unusual optical and electronic properties of transparent conducting oxides, attention has been paid to these materials for various applications. Titanium oxide (TiO_2) is a large bandgap semiconductor with interesting properties. It is transparent to visible light, has a high refractive index (at $\lambda = 550$ nm, $n = 2.54$ for anatase or 2.75 for rutile) and low absorption and consequently, it is widely used as an optical coating material [1, 2]. Also, it potentially has electronic device applications, such as dye sensitized photovoltaic cells, gas sensors, electrochromic and planar wave guides [3-5]. The dielectric constant of TiO_2 is high ($\varepsilon > 100$); therefore, it is suggested as an alternative for gate dielectrics to SiO_2 for memory and logic devices [6].

TiO_2 crystalizes in four polymorphic forms: anatase (tetragonal), rutile (tetragonal), brookite (orthorhombic) and β-TiO_2 (monoclinic) [7]. Anatase is the preferred phase for photo-induced applications, which justifies the research efforts put on its synthesis and on the study of its different properties. The photocatalytic application has been found to vary with its structural form and is reportedly higher in the anatase form compared to other forms [8-10].

A wide range of techniques have been used to prepare TiO_2 thin films, such as sputtering [11], electron beam evaporation [12, 13], pulsed laser deposition [14], chemical vapor deposition (CVD) [15] and sol-gel process [16]. However, it has been found that obtaining TiO_2 thin films, which are stable and have the properties required for the applications, is not always obvious. Indeed, the continuation of work on TiO_2 thin film preparation seems necessary. Therefore, the aim of the present work is to prepare post-deposition thermally oxidized TiO_2 thin films

Corresponding Author: I. M. Odeh **Email**: iodeh@yu.edy.jo

having good crystalline qualities with a reproducible process. Therefore, we have used Ion Beam Assisted (sputtering) Deposition (IBAD) technique to prepare our samples. To the best of our knowledge, this technique has not been used previously in a similar experiment, which motivated us to do this work.

Experimental Techniques

TiO_2 Thin Films Preparation

The substrates used were soda lime glasses of dimensions (25×8×1) mm^3; they were cleaned in an ultrasonic bath with acetone to remove any greasy traces, followed by alcohol and were then rinsed in running distilled water. Titanium thin layers of about 80 nm thickness have been deposited by simultaneous reactive DC sputtering and ion beam-assisted deposition (IBAD) technique. Fig.1 shows the actual setup and vacuum chamber during sample deposition.

We have used an End-Hall type ion beam source and a rotating substrate holder specifically designed, built and retrofitted to the vacuum chamber in such a way that ions from the source were directed to imping onto the rotating substrate holder at about 50–55 degrees during deposition.

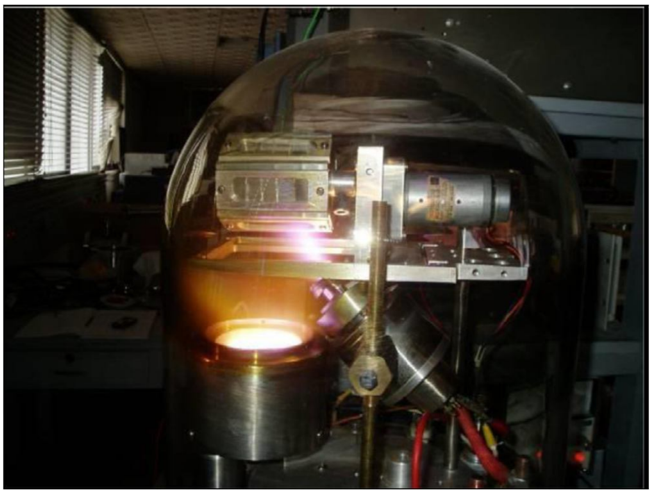

FIG. 1. Deposition set-up for the preparation of titanium thin films.

A low-tension high-current transformer supplied the necessary power to the W-filament of the ion source during deposition. An independent power supply (HP 6521A) supplied the accelerating voltages of 200–300 V applied to the ion source such that the ions leaving the source would have an energy of about 100–150 eV. A 75-mm DC magnetron sputtering accessory (Edwards, UK) fitted with a high purity target (Titanium) formed the main source of titanium atoms.

A novel substrate holder (Rotating Hexa-Holder) capable of loading six substrates simultaneously was designed and constructed specifically for this type of sample deposition, as shown in Fig. 1. The distance between the glass substrate and the source (Ti) target was kept at about 10 cm. A 1 kW DC power supply (MDX 1 K Magnetron Drive, Advanced Energy, USA) delivered the DC power to the water-cooled titanium target. Thoroughly cleaned glass substrates were used throughout this work. In addition to normal cleaning, glass substrates were bombarded with the ion source for five minutes prior to deposition to remove any traces from the surface. The films deposited were annealed at temperatures of 250°C, 350°C, 450°C and 550°C, for 2 hours. Annealing was conducted in a programmable MAGHMA THERM type oven.

TiO_2 Thin Films Characterization

The films structures was examined by BRUKER D8 diffractometer using Cu $K\alpha_1$ radiation (λ=1.5406 Å). Diffractograms were recorded from 10° to 90° with a step of 0.01°. The full width at half-maximum (FWHM) of the diffraction peaks was given directly by the X'Pert software program. The film thickness and axial roughness were checked by BRUKER Dektak XT type profilometer. AFM images were acquired using a Flex-Axiom Nanosurf system. Imaging was performed in phase contrast mode and image dimensions were 500 nm x 500 nm and 1000 nm x 1000 nm. Optical measurements have been carried out in the wavelength range 190 – 1100 nm, using a 210 SPECORD Plus UV-Visible spectrophotometer.

Experimental Results and Discussion

XRD Analysis

The structure of the films was determined by XRD, Figs. 2 and 3. The films without annealing crystallized in the Ti hexagonal structure, Fig. 2. The peaks are indexed using the ICDD card N° 44-1294. The peak at 47.606° is attributed to SiO_2 of the glass substrate referring to the ICDD card N°04-0379.

Fig. 3 shows XRD patterns of the films after annealing at 250 °C, 350 °C, 450 °C and 550 °C, for 2 hours.

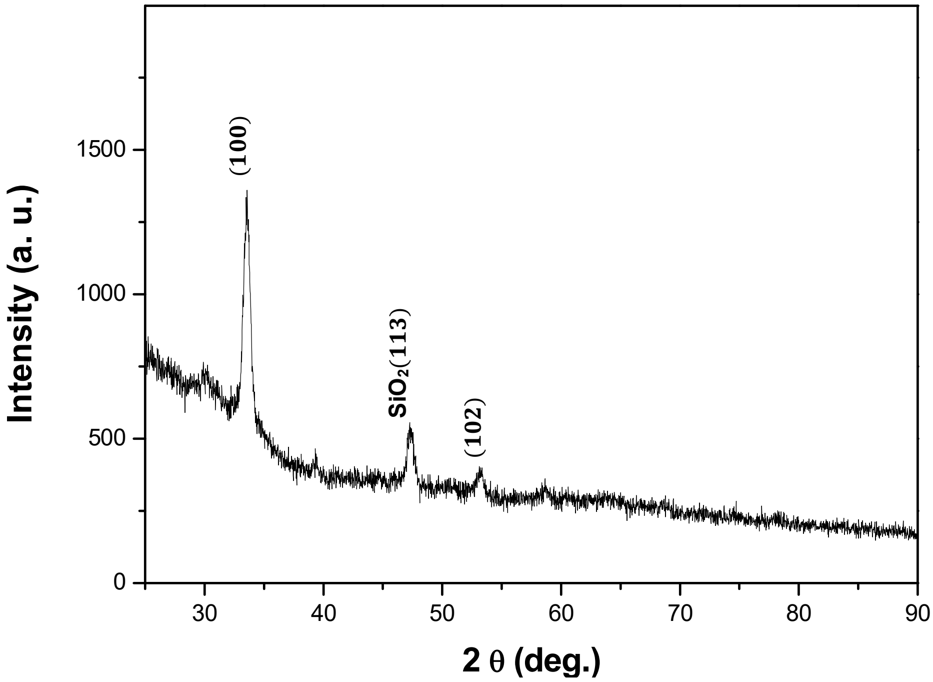

FIG. 2. XRD pattern of Ti thin film prepared by IBAD process.

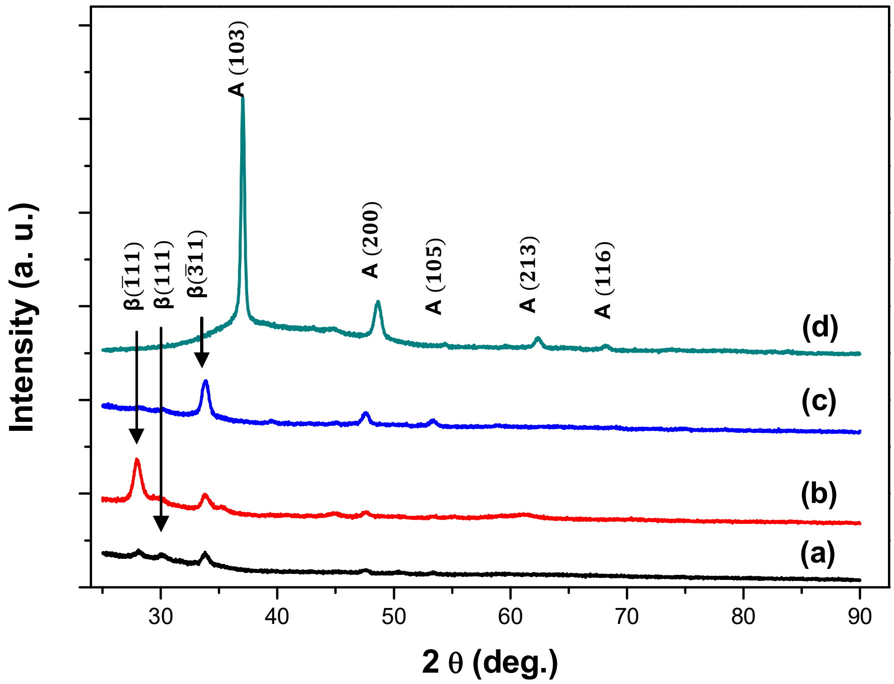

FIG. 3. XRD patterns of thin films obtained after annealing at 250°C (a), 350°C (b), 450°C (c) and 550°C (d), for 2 h.

Relationships used to deduce lattice parameters for hexagonal, monoclinic and tetragonal structure are respectively [17]:

$$\frac{1}{d_{hkl}^2} = \frac{4}{3}\frac{h^2 + hk + k^{2\,2}}{a^2} + \frac{l^2}{c^2} \qquad (1)$$

$$\frac{1}{d_{hkl}^2} = \frac{h^2}{a^2\sin^2\beta} + \frac{k^2}{b^2} + \frac{l^2}{c^2\sin^2\beta} - \frac{2hl\cos\beta}{ac\sin^2\beta} \qquad (2)$$

$$\frac{1}{d_{hkl}^2} = \frac{h^2 + k^2}{a^2} + \frac{l^2}{c^2} \qquad (3)$$

where a, c and β are lattice parameters and d_{hkl} is the reticular distance for the (hkl) plane family.

The average grain size D was calculated using Scherrer formula [18]:

$$D = K\,\frac{\lambda}{\beta\,cos\theta} \qquad (4)$$

where $K = 0.9$, $\lambda = 1.5406$ Å and β is the full width at half maximum (FWHM) of the diffraction peaks. β was calculated by Warren formula [19]:

$$\beta^2 = B^2 - b^2 \qquad (5)$$

where B is the measured peak width and b is the instrumental broadening, which is equal to 0.09° in this case.

ICDD card references, crystalline structure, lattice parameters and mean grain sizes deduced from different diffractograms are reported in Table 1.

TABLE 1. Crystalline parameters of thin films of Ti and TiO_2.

Thin film	ICDD card reference	Structure	Lattice parameters	Mean grain size $D\ (nm)$
Before annealing	44-1294	Hexagonal	$a = 2.990$ Å $c = 4.515$ Å	26
Annealed at 250°C for 2h	46-1238	Monoclinic	$a = 12.163$ Å $b = 3.735$ Å $c = 6.513$ Å $\beta = 107.29°$	29
Annealed at 350°C for 2h	46-1238 and 21-1272	- Monoclinic - Tetragonal Anatase type (105)	$a = 12.163$ Å $b = 3.735$ Å $c = 6.513$ Å $\beta = 107.29°$ $a = b = 3.741$ Å $c = 9.582$ Å	28 20
Annealed at 450°C for 2h	46-1238 and 21-1272	- Monoclinic - Tetragonal Anatase type (105)	$a = 12.163$ Å $b = 3.735$ Å $c = 6.513$ Å $\beta = 107.29°$ $a = b = 3.741$ Å $c = 9.582$ Å	28 20
Annealed at 550 °C for 2h	21-1272	Tetragonal Anatase type	$a = b = 3.741$ Å $c = 9.582$ Å	28

A phase transition between monoclinic β -TiO_2 structure and tetragonal anatase structure is observed when the annealing temperature is increased from 250 °C to 550 °C. The grain size is not affected by the increase of annealing temperature. The presence of the two structures at the intermediate temperatures 350 °C and 450 °C confirms this transition. The transformation of the structure from monoclinic to tetragonal under the effect of temperature means a transition to a more ordered structure. Therefore, the crystallinity seems to improve with annealing temperature. This is explained by the fact that on annealing at elevated temperatures, atoms acquire high enough ability to organize themselves in a more crystalline arrangement [20, 21].

AFM Visualization

Images of TiO_2 thin film surfaces were taken at scan ranges of 500 nm and 1000 nm, Figs.4 and 5. The values of roughness parameters as the arithmetic mean height Sa, the root-mean-square height Sq, the maximum height Sz, the maximum peak height Sp and the maximum pit height Sv, are reported in Table 2.

The surface roughness of the sample annealed at 550°C (4.48 nm rms) slightly increased compared to the one annealed at 250°C (3.01 nm rms). This is also reflected by the mean height of the analyzed grains (2.19 nm *vs*. 2.01 nm). The phase contrast is strong at grain boundaries. This contrast might be due to crosstalk with topographic features.

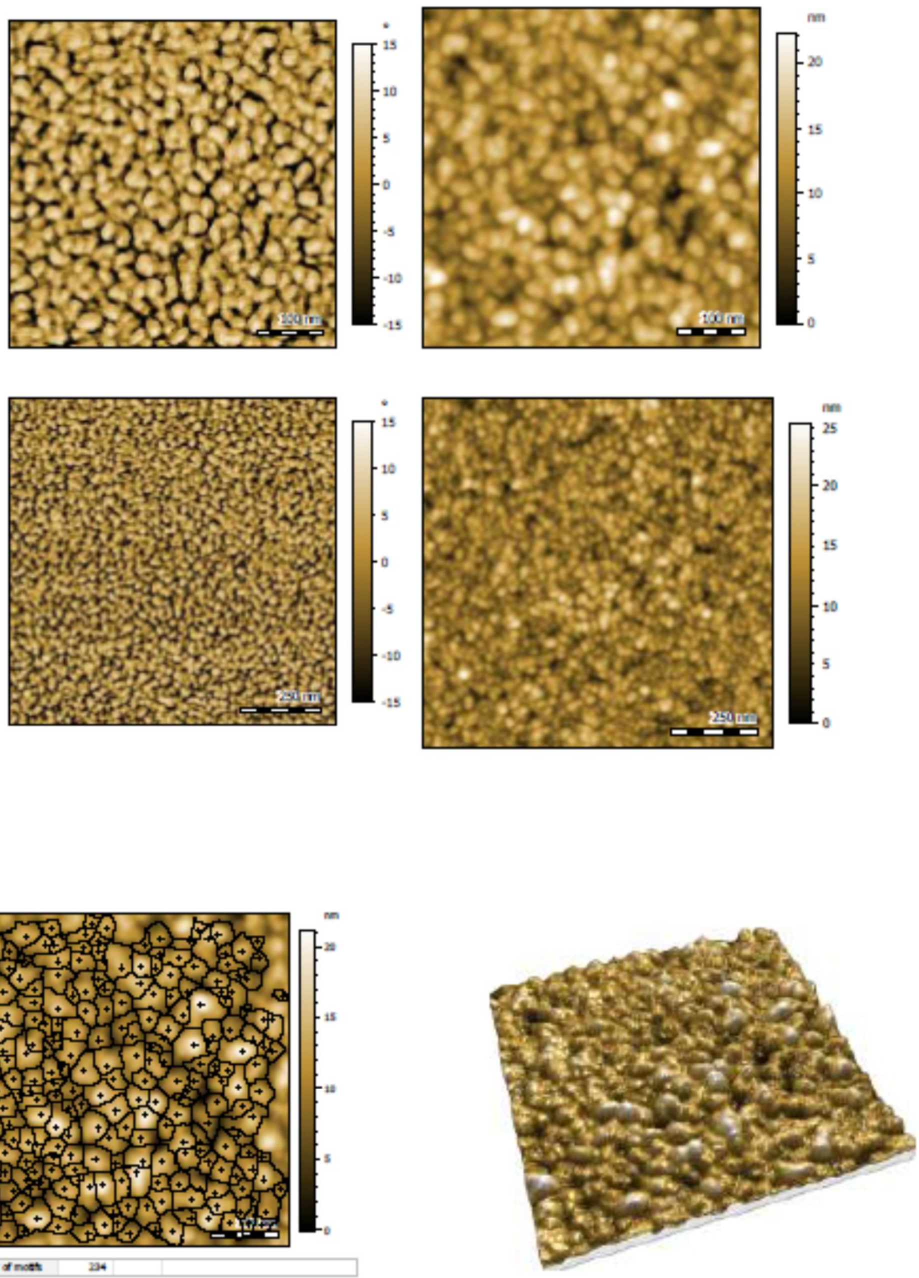

Number of motifs	234		

Parameters	Stat.	Value	Unit
Height	Mean	2.01	nm
	Std dev	1.66	nm
Area	Mean	874	nm²
	Std dev	457	nm²
Nb of neighbors	Mean	5.84	
	Std dev	1.55	
Mean diameter	Mean	29.5	nm
	Std dev	8.58	nm

FIG. 4. AFM images for TiO_2 thin film obtained after annealing at 250°C for 2 h.

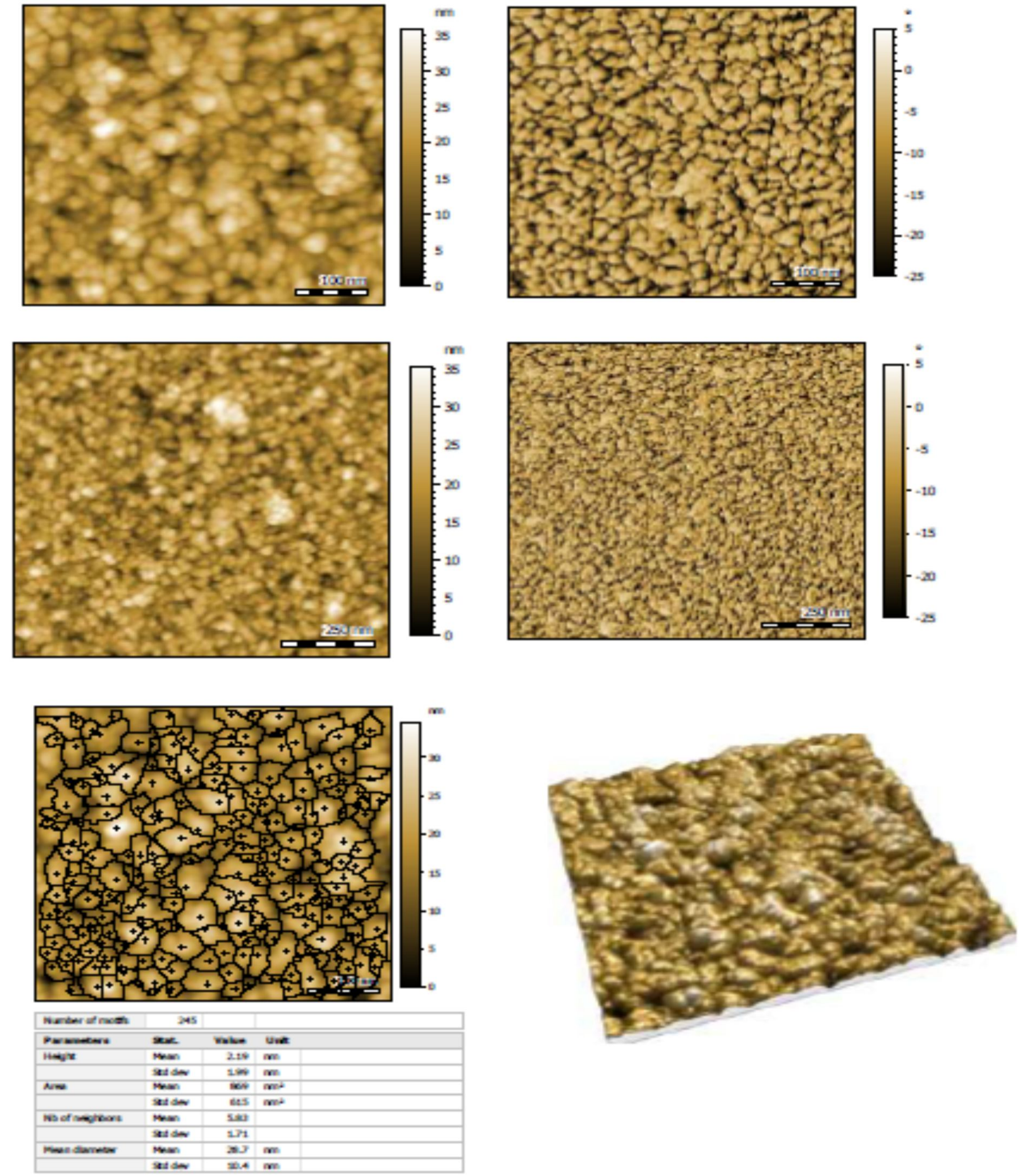

FIG. 5. AFM images for TiO_2 thin film obtained after annealing at 550°C for 2 h.

TABLE 2. Roughness and grain parameters of TiO_2 thin films obtained after annealing for 2 h at 250 °C and 550 °C.

Thin film obtained at roughness and grain parameters	250 °C	550 °C
Sa (Arithmetic Mean Height) (nm)	2.38	3.58
Sq (Root Mean Square Height) (nm)	3.01	4.48
Sz (Maximum Height) (nm)	22.20	36.00
Sp (Maximum Peak Height) (nm)	11.20	17.60
Sv (Maximum Pit Height) (nm)	11.10	18.40
Mean Grain Size (nm)	29.96	28.80
Mean Number of Grain Neighbors	5.84	5.83

Optical Measurements

Optical transmittance, Fig. 6, absorption coefficient, Figs. 7 and 8 and optical energy gap, Fig. 9, of thermally oxidized Titanium films have exhibited high transmission of 85 - 90% in the wavelength range of 300 – 800 nm and wide energy gap, in agreement with published data.

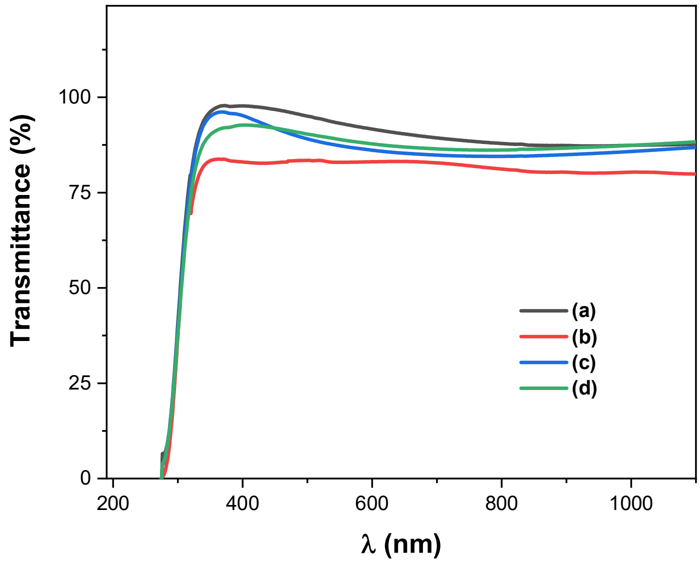

FIG. 6. Transmittance spectra *versus* wavelength for thin films obtained at 250°C (a), 350°C (b), 450°C (c) and 550°C (d), for 2 hours.

The results of the absorption coefficient calculation for different samples are provided in Figs. 7 and 8. From the transmission spectra and the thickness determined by the profilometer, we calculated the absorption coefficients using the following relation [22]:

$$\alpha = \frac{1}{d}\, ln\left(\frac{100}{T\ (\%)}\right), \tag{6}$$

where d is the film thickness and T is the transmittance.

In the low-energy region of the incident photon (1–2.75 eV), we see a decrease in the absorption coefficient. Considering the annealing temperature, we have found that the optical absorption coefficient increases when the temperature goes from 250 °C to 350 °C and then decreases for the temperatures 450 °C and 550°C.

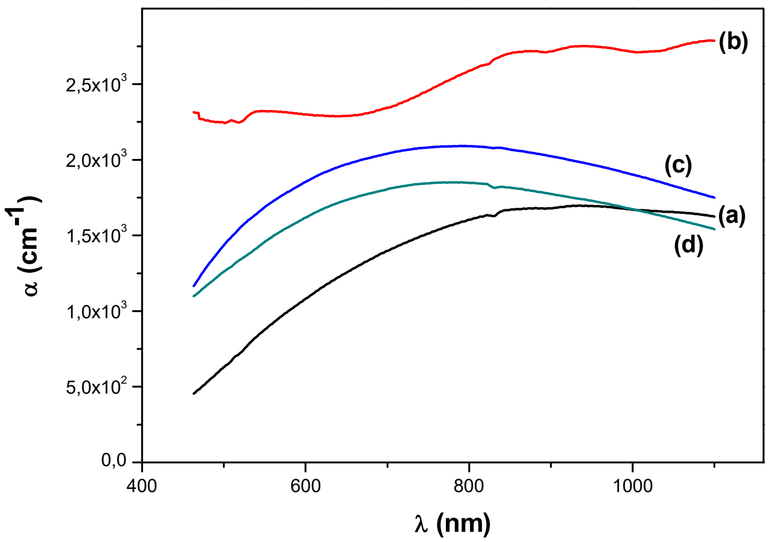

FIG. 7. Optical absorption coefficient *versus* wavelength for thin films obtained after annealing at 250°C (a), 350°C (b), 450°C (c) and 550°C (d), for 2 hours.

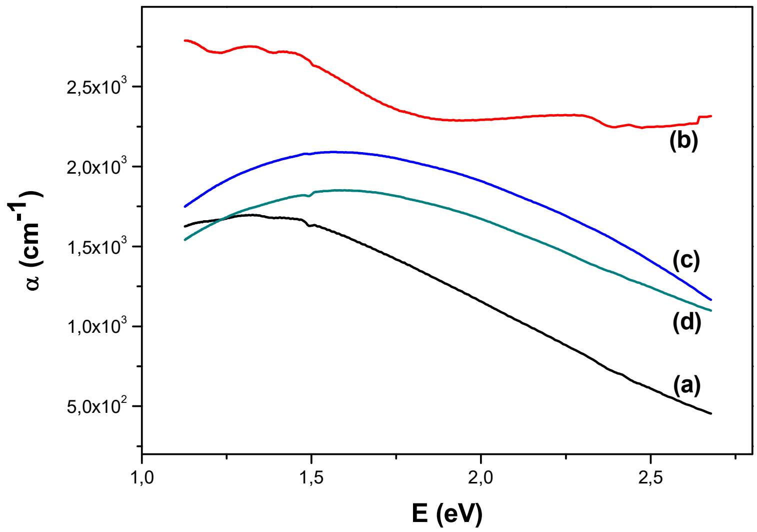

FIG. 8. Optical absorption coefficient *versus* photon energy for films after annealing at 250°C (a), 350°C (b), 450°C (c) and 550°C (d), for 2 hours.

The optical band gap energy of TiO_2 thin films annealed at 250°C and 550°C was calculated from the absorption spectra using the Tauc formula [23]:

$$(\alpha h\nu) = A\left(h\nu - E_g\right)^n, \tag{7}$$

where α is the absorption coefficient, $h\nu$ is the photon energy, A is a constant, Eg is the optical band gap and n is a number equal to 2 and 1/2 for indirect and direct allowed transition, respectively. Knowing that TiO_2 is an indirect gap material [24, 25], the optical band gap values are obtained by extrapolating the linear part of $(\alpha h\nu)^{1/2}$ curves to α=0, as shown in Fig.9.

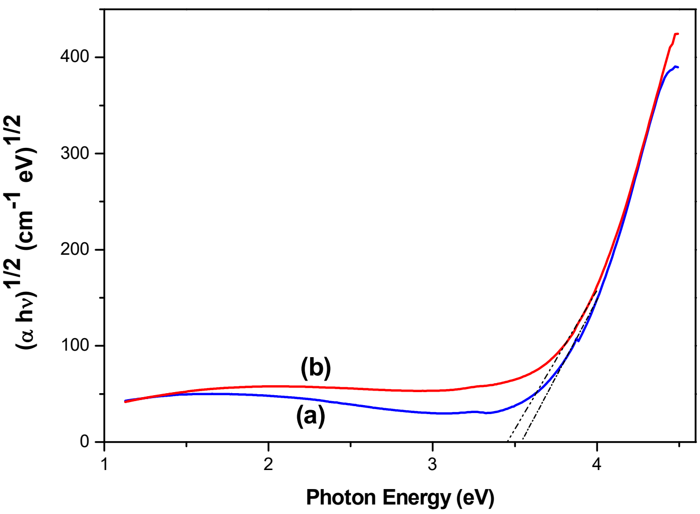

FIG. 9. Plots of $(\alpha\, h\nu)^{1/2}$ versus photon energy for thin films obtained after annealing at 250°C (a) and 550°C (b), for 2 hours.

The results of the optical analysis were interpreted in light of the crystalline properties deduced from the structural characterization of the different samples. The TiO_2 thin films with monoclinic β-TiO_2 and tetragonal anatase structures, obtained by annealing at 250 °C and 550 °C for 2 h, respectively showed better transmittance, Fig.6 and low absorption, Figs.7 and 8, compared to those of TiO_2 thin films having two phases resulting from annealing at 350 °C and 450 °C for 2 h. This leads to the conclusion that the optical absorption increases and the optical transmittance decreases, when the crystalline order is improved.

The obtained values of indirect optical band gap are 3.43 eV and 3.61 eV for thin films annealed at 250°C and 550°C, respectively. Certainly, the most cited value for anatase phase is 2.23 eV [21], but other works have obtained values comparable to ours [24, 25].

Conclusion

In this work, we have successfully prepared thin films of sputtered titanium using ion beam-assisted deposition (IBAD). The films were thermally oxidized and successfully annealed at temperatures of 250°C, 350°C, 450°C and 550°C. XRD spectra have shown that the film phase was modified from the monoclinic type to the tetragonal type by increasing the annealing temperature from 250 °C to 550 °C. Height parameters deduced from roughness AFM analysis have noticeably increased as a result of thermal oxidation at higher temperatures. Optical measurements indicate high transmission films over the visible range and a wide optical energy gap in the range 2.43-3.61 eV.

Acknowledgements

The authors are grateful to Dr Ch. Bippes and Dr. R. Djaafar (Nanosurf AG, Switzerland) for the AFM visualization of our samples.

References

[1] Martinu, L. and Poitras, D., J. Vac. Sci. Technol. A, 18 (2000) 2619.

[2] Wang, Z., Helmersson, U. and Kall, P.O., Thin Solid Films, 405 (2002) 50.

[3] O'Regan, B. and Grätzel, M., Nature, 353 (1991) 737.

[4] Saveninije, T.J., Warman, J.M. and Goosens, A., Chem. Phys. Lett., 287 (1998) 148.

[5] Montesperelli, G. and Pumo, A., Sens. Actuators B, 24–25 (1995) 705.

[6] Kingon, I., Maria, J.-P. and Streiffer, S.K., Nature, 406 (2000) 1032.

[7] Borlaf, M., Colomer, M.T., Moreno, R. and Ortiz, A.L., Journal of the European Ceramic Society, 34 (2014) 4457.

[8] Sen, S., Mahanty, S., Roy, S., Heintz, O., Bourgeois, S. and Chaumont, D., Thin Solid Films, 474 (2005) 245.

[9] Tsai, S.J. and Cheng, S., Catal. Today, 33 (1997) 227.

[10] Maruska, H.P. and Ghosh, A.K., Sol. Energy, 20 (1978) 443.

[11] Tang, H., Prasad, K., Sanjines, R., Schmid, P.E. and Levy, F., J. Appl. Phys., 75 (1994) 2042.

[12] Guang-Lei, T., Hong-Bo, H. and Jian-Da, S., Chin. Phys. Lett., 22 (2005) 1787.

[13] Oh, S.H., Kim, D.J. and Hahn, S.H., Mater. Lett., 57 (2003) 4151.

[14] Kim, J.H., Lee, S. and Im, H.S., Appl. Surf. Sci., 151 (1996) 6.

[15] Campbell, S.A., Kim, H.S., Gilmer, D.C., He, B., Ma, T. and Gladfelter, W.L., IBM J. Res. Dev., 43 (1999) 383.

[16] Wang, Z., Helmersson, U. and Käll, P.O., Thin Solid Films, 405 (2002) 50.

[17] Kaeble, E.F., "Handbook of X-rays", Ed., (Mac Graw Hill, 1981).

[18] Sherrer, P., Götinger Nachrichten, 2 (1981) 98.

[19] Warren, B.E., J. Appl. Phys., 12 (1941) 3750.

[20] Fallah, H.R., Ghasemi, M. and Hassanzadeh, A., Physica E, 39 (2007) 69.

[21] Khan, A.F., Mehmood, M., Durrani, S.K., Ali, M.L. and Rahim, N.A., Mater. Sci. in Semic. Process, 29 (2015) 161.

[22] Palik, E.D., "Handbook of Optical Constants of Solids", Ed., (Academic Press, San Diego, 1998).

[23] Tauc, J., "Amorphous and Liquid Semiconductors", Ed., (Plenum Press, New York, 1974).

[24] Wang, Z., Helmersson, U. and Kall, P.O., Thin Solid Films, 405 (2002) 50.

[25] Sen, S., Mahanty, S., Roy, S., Heintz, O., Bourgeois, S. and Chaumontet, D., Thin Solid Films, 474 (2005) 245.